

BEAM MEASUREMENTS ON THE FIRST TANK OF LAMPF*

D. A. Swenson, B. C. Goplen, M. A. Paciotti and J. E. Stovall
University of California
Los Alamos Scientific Laboratory
Los Alamos, New Mexico 87544

A variety of measurements have been made on the beam in the first tank of LAMPF. The results of these measurements are compared to the expected results based on beam dynamics calculations. The properties investigated include the transverse admittance of the linac, the transverse emittance of the injected and accelerated beam, momentum spectra as a function of tank excitation (field amplitude), and the performance of the single and double buncher systems. Some of the techniques used in the measurements are described.

Introduction

The first portion of LAMPF has been operated as an accelerator for a period of seven months. This portion includes the Cockroft-Walton voltage source, the proton ion source, the accelerating column, the low-energy beam transport system, the double buncher system and the first tank of the drift-tube linac. The purpose of this initial operation was to perfect the performance of this critical portion of LAMPF, and to test the validity of the dynamics calculations used in the design of the linac.^{1,2} The performance of the ion source, accelerating column, and low-energy transport system are described in the proceedings of this³ and recent⁴ accelerator conferences. The performance of the double buncher system and the first tank of the linac are described in this paper and in the literature.⁵

The first tank of LAMPF is 11 ft long and contains 31 drift tubes. It accelerates the .75 MeV injected beam of protons to an energy of 5.39 MeV. The system is designed for a peak current of 17 mA at a duty factor of 6%, yielding an average beam current of 1 mA. The tank requires an excitation of 300 kW to achieve the design field gradients, which increase linearly from 1.6 MV/m at the entrance end to 2.3 MV/m at the other end. Field measurements show the field distribution to be within 1.4% of design except for the end cells.⁶

The low-energy transport system includes a unique double-buncher system, the purpose of which is to shape the longitudinal phase space of the beam so that a greater fraction of the beam is accepted by the accelerator.⁷ Both cavities operate at the fundamental frequency (201.25 MHz) of the drift-tube linac. They are located 7 and 1.5 m upstream from the linac tank. The first cavity requires only a few watts of excitation and acts as a pre-buncher for the second cavity, or main buncher, which requires approximately 160 W of excitation.

The main experimental gear consisted of emittance measuring hardware and a spectrometer magnet. The emittance hardware, which is described more fully in a later section, was used to measure transverse emittance, form slits and pinholes, and in general, to tune the low-energy transport system.

Located downstream from tank 1 was a 180° double-focusing spectrometer of high resolution. It was used to discriminate against low-energy tails in measuring transmission and to measure the energy spectrum.

Most of the measurements reported here were made with the aid of a small digital computer (Data General's NOVA) interfaced with a prototype of the

LAMPF data acquisition and control terminal (DACT).⁸ This system can operate relays, drive stepping motors and acquire data through the terminal. The mini-computer can process the data and display it either on a storage oscilloscope (Tektronics 611) or on a teletype.

Transverse Admittance of the Linac

The transverse admittance of tank 1 was measured experimentally by scanning the entrance of the tank with a pencil beam. This beam was created by forming two 30 mil square pinholes on the beam axis separated by 1.8 m. The position and angle of the beam at the tank entrance were varied with two sets of steering magnets, and resulting current through the linac measured. Experimental results are presented on the left side of Fig. 1, representing the phase space admittance transformed to the surface of the first quadrupole magnet in the tank. Smooth contour lines have been drawn through approximately 100 data points in each plane. Position of the beam was measured to an accuracy of ± 15 mils. The angular error is $\pm 15\%$ because of uncertainty in the magnetic fields of the steering magnets. Due to a low signal level, transmission currents were read to $\pm 15\%$.

This experiment was simulated theoretically using the PARMILA beam-dynamics program; results are shown on the right side of Fig. 1. The presence of contour lines, rather than a hard-edged admittance, reflects integration over the coupled longitudinal phase space, as well as the effect of finite beam size and divergence. These calculations assume perfect linac alignment.

The shape and orientation of the measured and calculated admittances are then in excellent agreement. The area of the measured admittance is smaller than the area of the calculated admittance in both planes. Studies on the effects of quadrupole misalignments show that random 5 mil quadrupole misalignments reduce the

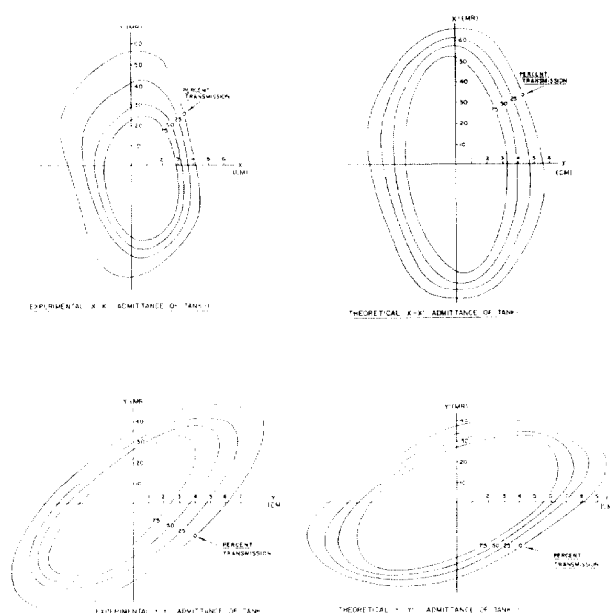


Fig. 1 Linac admittance, measured and calculated.

*Work performed under the auspices of the U. S. Atomic Energy Commission.

transverse admittance of the first tank by 30 - 50%. The difference must reflect an actual reduction of the linac admittance as a result of random quadrupole misalignments on the order of 5 mils in magnitude.

This measurement is particularly interesting since it provides a measurement of the transverse properties of the tank itself, independent of the transverse properties of the available beam. It will be repeated periodically in an effort to detect changes in the quadrupole alignment or excitation.

Transverse Emittance of the Beam

Three sets of hardware for measuring the transverse emittance of the beam in both the horizontal and vertical planes were installed along the beam line. One set was installed near the ion source and the other two sets were installed near the entrance and exit of the tank. Each set consisted of four jaws and two collector strip assemblies mounted on separate linear actuators. Two jaws set to form a slit and one collector assembly are used for the emittance measurement in each plane. The strip electrodes on the collector assembly and the slit are normal to the plane of interest. The collector assembly has 38 strip electrodes spaced 20 mils center-to-center, and is located about 1 m downstream from the slit.

During the measurement, the mini-computer drives the jaws and collectors through the beam in 100 steps of 10 mils each. After each step, the signals from the 38 strip electrodes are collected, and processed to reveal the angular properties of the beam at that position of the slit.

Displays created from these data are shown in Figs. 2 to 5. The transverse phase space is shown in an isometric projection at the bottom of the display, with the transverse coordinate horizontal and the transverse angular coordinate at 45°. The portions of the transverse phase space occupied by beam are shown in the apparent third dimension.

The upper left-hand part of the display is the normal two-dimensional view of the transverse phase space, where the shaded area corresponds to region of phase space in which the beam density is greater than a given threshold. Tucked into the left-hand corner of this graph is the emittance distribution graph. It gives the percentage of the beam current (0 - 100%) lying outside a given intensity contour line as a function of the phase space area (10 π cm mrad at center of Fig.) within this contour line. The upper right-hand

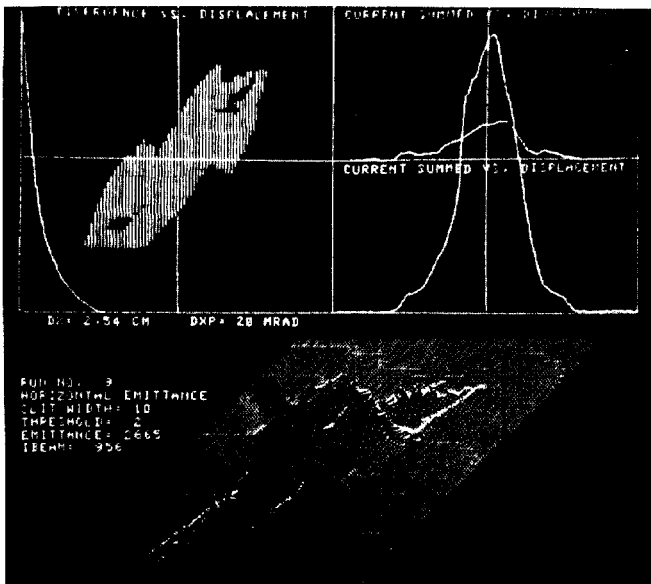


Fig. 2 Horizontal emittance at tank 1 entrance.

part of the display consists of two beam profile curves.

Properties of Beam Into Linac

The transverse properties of the beam normally used for injection into the linac with bunchers off are shown in Figs. 2 and 3. The total emittance reported on these measurements is 2.7 π cm mrad in the horizontal plane and 3.1 π cm mrad in the vertical plane. The emittance distribution graphs on these figures indicate that 90% of the beam lies within 1.4 π cm mrad and 1.6 π cm mrad respectively.

Similar sets of measurements indicate that excitation of the bunchers increases the transverse emittance to 2.9 π cm mrad and 3.5 π cm mrad respectively, representing an average increase of about 10% for the two planes.

The transport system is designed to transport the beam from the ion source to the linac, preserving circular symmetry in the long drift spaces, producing double waists at certain locations such as the buncher cavities, and delivering a beam that is "matched" to the linac. Quadrupole excitations in the transport system corresponding to minimum beam loss differed significantly from the design excitations. Consequently, the phase space orientation of the beam at the emittance measurement near the entrance to the linac also differed significantly from that of the design beam. Efforts to achieve the design orientation of the beam at the location of the emittance measurement were unsuccessful.

There are four quadrupole lenses between the location of the emittance measurement and the entrance to the linac. Using the phase space orientations shown in Figs. 2 and 3 as input to the PARMILA program, runs were made to find a set of excitations for the four lenses that would match the existing beam to linac. No solution was found. The closest approach, however, gave excitations in excellent agreement with those obtained empirically in optimizing transmission through the tank. Subsequent operation was with the calculated excitations corresponding to the closest approach to the matched condition. Dynamics calculations reveal that the failure to match the beam to the linac resulted in peak transverse oscillations that were 40% larger than present in the matched beam.

Properties of Beam Out of Linac

The transverse properties of the beam normally emerging from the linac with bunchers off are shown in Figs. 4 and 5. The total emittance reported on these

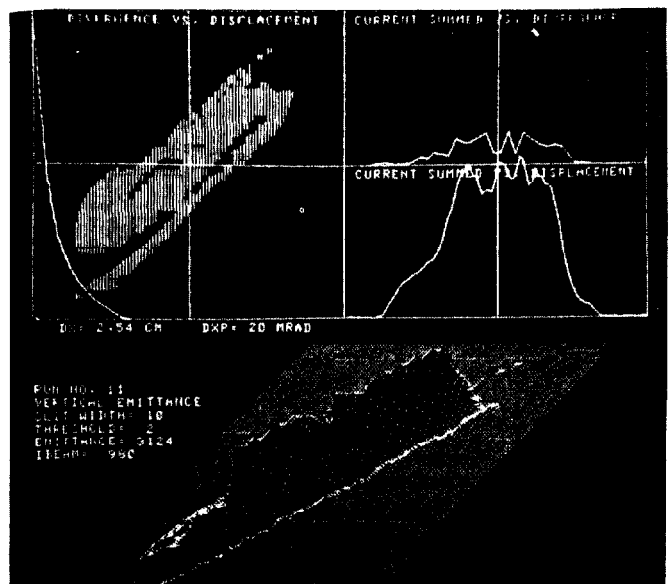


Fig. 3 Vertical emittance at tank 1 entrance.

measurements is $.9 \pi$ cm mrad in the horizontal plane and 1.0π cm mrad in the vertical plane. These values are quite consistent with the emittance of the injected beam divided by the adiabatic damping factor of 2.7.

If it is true that none of the injected beam within the longitudinal acceptance of the linac is lost radially, there is no evidence of growth in the effective emittance of the beam as a result of acceleration. If, on the other hand, 10% of the injected beam was lost radially, the indicated emittance growth factor could be as high as 1.7. Transmission measurements reported below suggest that little or none of the injected beam within the longitudinal acceptance of the linac is lost radially, which, in turn, implies that the emittance growth factor resulting from acceleration to 5 MeV is close to unity.

Due to the short length of the linac tank, some of the beam, destined to be lost, emerges from the tank as a low-energy component. Evidence of a different component of the beam can be seen in Figs. 4 and 5. Experiments with steering magnets confirm this component to be lower in energy to the main component of the beam.

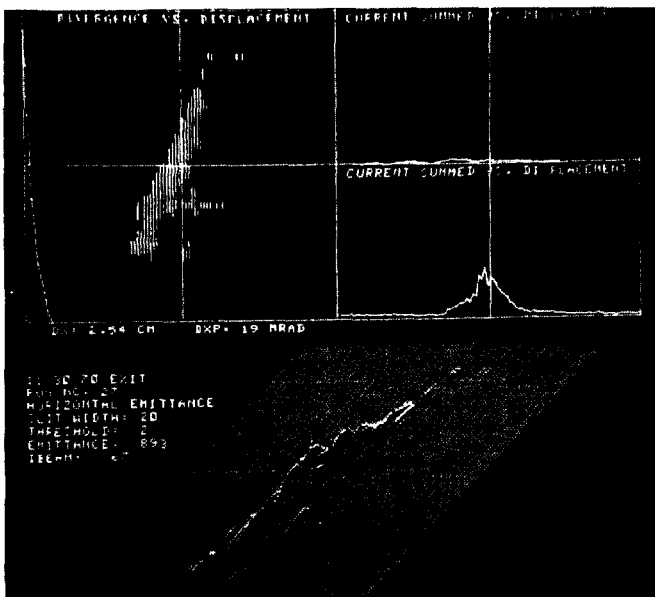


Fig. 4 Horizontal emittance at tank 1 exit.

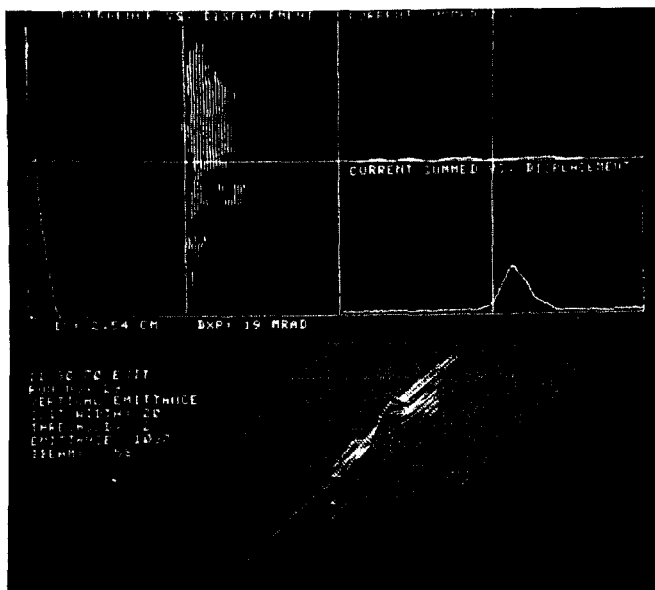


Fig. 5 Vertical emittance at tank 1 exit.

Transmission Measurements

The transmission of tank 1 was observed over the entire running period as a prime measure of performance. Transmission is defined here to be the ratio of accelerated current to the current injected into the tank.

Transmission vs Tank Excitation

Figure 6 gives the measured and calculated transmissions for unbunched, single bunched, and double bunched beams as a function of tank excitation. The entire transverse emittance of the beam was used for these measurements. The error bars on the data indicate errors in the measurement of the current into the tank. The accelerated current was read on a copper plate in the focal plane of the spectrometer. The plate was biased with +70 V, and the bias curve was flat beyond +30 V.

Since no absolute measure of tank field was made, the transmission curves serve as a way of determining the design excitation. The data are plotted so as to make the theoretical and experimental thresholds with no bunchers coincide. Relative tank amplitudes are known to .25% using the signals from 5 loops in the tank into calibrated crystals whose outputs are read on a calibrated oscilloscope. This convention establishes the design tank excitation. Other conventions are possible as can be seen in the next section.

Transmission Using Both Bunchers

In this experiment, the phase of the main buncher was first determined by measuring the transmission of the beam through the spectrometer with the pre-buncher off. Since the experimental curves agreed closely with calculations, this curve was used to set the main buncher at its design phase. The pre-buncher was then phased to maximize transmission. The two bunchers were then driven together in phase to produce the plot on the left in Fig. 7. The phase scale on the data is positioned roughly to match the calculation. The width of the scale is known accurately from trombone lengths. The maximum transmission was $80\% \pm 15\%$.

In the corresponding theoretical calculation, particles were considered transmitted if above 5 MeV in energy. Results of the calculation are shown on the right in Fig. 7. The use of measured tank fields⁶ in the calculation was found to be a significant factor in achieving this agreement between theory and experiment.

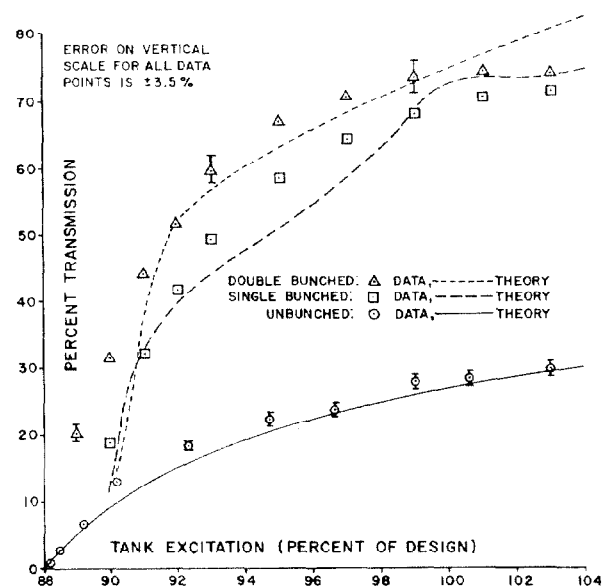


Fig. 6 Transmission vs tank 1 excitation.

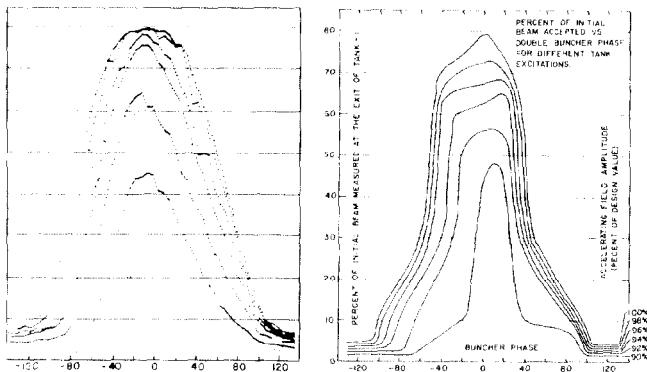


Fig. 7 Transmission as function of buncher phase and tank excitation, measured and calculated.

Momentum Spectra

Measurement of the momentum spectrum of the beam as a function of tank excitation offers some of the most detailed information available on the behavior of the longitudinal phase space. The results of the measurements of the spectra for unbunched, single bunched, and double bunched beams are compared with the results of computer calculations.

Experimental Details

The 180° double-focusing spectrometer was located 1.7 m from the end of the tank. A quadrupole doublet located midway between the tank and the spectrometer contained the beam sufficiently so that the entire transverse phase space of the accelerated beam was accepted by the spectrometer and reached the focal plane. The complete spectrum is taken on one beam pulse using an array of 38 collecting strips on the focal plane connected to 38 sample and hold circuits which store the data.

The dispersion of the spectrometer is 1.9 cm per percent in $\Delta p/p$. The resolution of the array of 3 mm wide strips in the focal plane is $\Delta p/p = .16\%$. The resolution of the spectrometer with the beam spot size used is $\Delta p/p = .1\%$. The data were taken with a 60 mil square pinhole before the tank, resulting in a small enough spot size in the dispersion plane of the spectrometer so that no slits were required after the tank.

Data Collection

Figure 8 is an isometric plot which contains a complete survey of momentum information with bunchers off. Each horizontal trace is the momentum spectrum for a different tank excitation. The tank excitation scale is based on the previous section. One-hundred-fifty spectra make up the plot. Successive runs of the same plot are almost indistinguishable. The line at the left of the isometric plot is the integrated current at each RF level. It shows the proper increase of total transmission with increasing tank field.

Calibrations

The energy scale was established by calibrating the spectrometer with the .75 MeV test beam that was drifted through the tank with RF off. The .75 MeV beam energy was found with a voltage divider. Measurements on the voltage divider resistors for the Cockroft-Walton give an error of about ± 150 V on the proton energy. The uncertainty in reading the high voltage drop due to beam loading is about ± 200 V. Aside from unknown systematics, the injector energy is known to $\pm .04\%$

The momentum corresponding to another spectrometer current is deduced by scaling the results of the .75 MeV runs. The uncertainty in determining which wire corresponds to design momentum at the current used

for all runs is about ± 1 wire or $\pm .3\%$ in energy.

The dispersion was measured at the focal plane with both the .75 MeV beam and the 5 MeV beam. It has a small linear dependence on the position at the focal plane. The error in the dispersion at any place on the focal plane is $\pm 5\%$. Consequently, energy widths are known to 5%.

Comparison of Measurements and Calculations

Figure 9 shows a theoretical result to be compared with the data in Fig. 8. The calculation was done for an axial unbunched beam without space-charge effects. Other calculations done at design RF level have shown that the spectrum of the entire transmitted beam is independent of injection position and angle. The momentum data in Fig. 8 is for the entire transmitted beam.

Comparison of Tank Excitation and Energy Scales. Above 94% excitation, data and calculation (Figs. 8 and 9) are similar except for systematic scale shifts.

The distinct features in the data appear 1% higher in field than the same features in the calculations. Sliding the tank excitation scale on the data brings all of the main features above 94% on Figs. 8 and 9 into coincidence. This method of fixing the excitation scale is an alternative to sliding the scales to match at threshold. The two results differ by 1%, thus leading to a 1% uncertainty in the determination of the design excitation.

The measured beam energy for excitations above 94% is 1.1% higher than the calculated value. An upper limit on the energy oscillation in the data as tank excitation increases is estimated to be .5% for the region above 94%. Therefore, a maximum of one-half of the 1.1% energy discrepancy could be attributed to a phase oscillation. The effect is in the direction that would be caused by saturation. However, the field in the spectrometer is only 8 kG, and measurement of the field integrals was not attempted. The required accuracy would be better than .5% to see a 1% energy error.

Comparison of the Shapes of the Spectra. Aside from the above-mentioned scale shifts, there is remarkable similarity between data and calculations above 94%. It is not known why the computer does not produce the observations below 94%. With near certainty, the tailing off of beam energy below 94% tank fields is not instrumental.

Energy widths measured from single spectra at several tank excitations all appear wider than the computed spectra by roughly 5 - 10%. Accuracy is limited by the coarseness of the collecting grid. This shift is at the limit of energy width uncertainty, which was $\pm 5\%$, and therefore cannot be claimed to be real.

The spectrum vs excitation plots for the single buncher (Figs. 10 and 11) and double buncher (Figs. 12 and 13) give equally interesting comparisons. In the case of the double buncher, the very steep ridge between 95% and 101% field is evident in data and theory. Pre-buncher field amplitudes 25% on either side of the field for Fig. 13 caused the ridge to separate into two distinct peaks.

The sensitivity of the shape of the momentum spectrum to various parts of the calculation has not been investigated. The agreement for no bunchers above 94% excitation is so good that we assert that the longitudinal phase space calculation is valid and independently that the linac is performing as designed. If agreement were less than perfect, one would not know whether to attribute the discrepancy to failure in the dynamics calculation or failure of the accelerator to reproduce the design model.

Correlation of Output Energy With Transverse Coordinate

A particularly troublesome aspect of the momentum measurement, until it was understood, was the

presence of a strong correlation between the momentum spectrum and the output transverse coordinate. As noted above, transverse oscillations within the linac do not have much effect on the energy spectra of the entire accelerated beam, but they can produce the observed energy-spatial correlations. When a beam is injected with a transverse oscillation, coupling to the longitudinal dynamics will make the position and angle of the emerging beam depend on the phase at which it entered the linac. Since the output energy is directly dependent on the entrance phase, there results a strong correlation between the energy spectrum and the output transverse coordinate when the beam has a significant transverse oscillation in the early part of the linac.

Horizontal and vertical slits were formed at the exit of the linac and the spectrum was measured as a function of slit position. The correlation was most pronounced in the vertical plane. The PARMILA dynamics program was arranged to produce the energy spectrum as a function of "slit position" for different "injected" transverse oscillations. The correlation calculated for a beam injected with no displacement and a +10 mrad angular error in the vertical plane is in remarkable agreement with the data.

Acknowledgments

The operation and measurements reported here were the result of a superb effort on the part of a large number of the people in the Meson Physics Division. The Operations Section, set up during the effort, performed smoothly and efficiently. Without their help, these measurements could not have been completed. Thanks go to Bill Shlaer for the able assistance he gave during the last two months of the run. Ralph Stevens, Ken Crandall and Dick Tregellas were particularly generous with their time and talents. The expertise of Bob Jameson, Ed Schneider, Don Machen, Ross Faulkner, Jack Hardwick and Paul Allison are highly valued. The repeated help of Harold Lederer, Joe Ortega, Leonard Scott and Tom Lopez is gratefully acknowledged. Morris Engelke and his staff of monitors were most cooperative. The authors are indebted to many for the privilege of publishing these results.

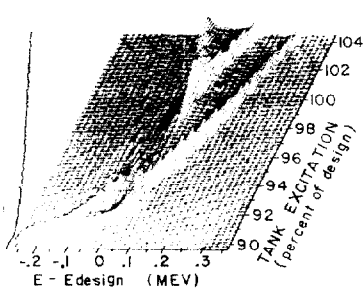


Fig. 8 Measured momentum spectra, bunchers off.

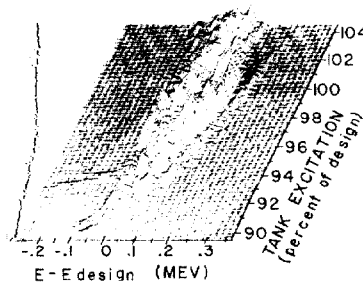


Fig. 10 Measured momentum spectra, single bunched.

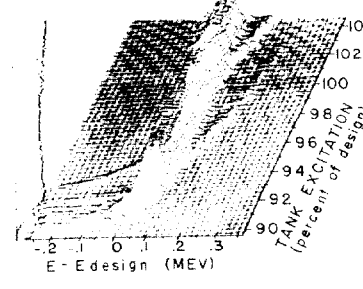


Fig. 12 Measured momentum spectra, double bunched.

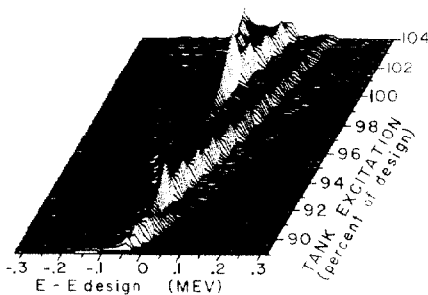


Fig. 9 Calculated momentum spectra, bunchers off.

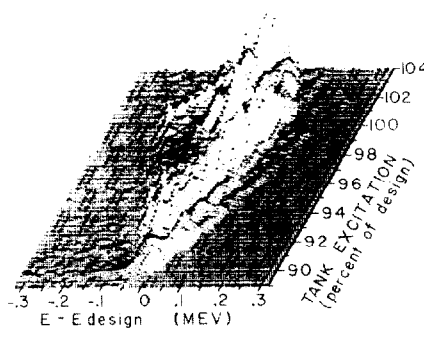


Fig. 11 Calculated momentum spectra, single bunched.

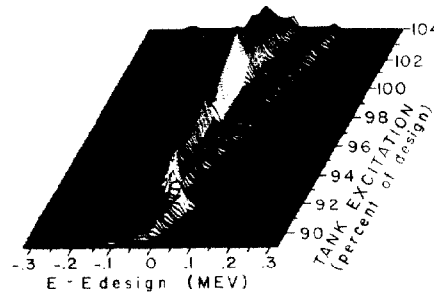


Fig. 13 Calculated momentum spectra, double bunched.

References

- ¹ D. A. Swenson, "Generation of Geometrical Dimensions for Drift Tube Linacs," LASL memo MP-3/DAS-1, June 29, 1967 (unpublished).
- ² J. E. Stovall, "Beam Dynamics Diagnostic Measurements in Tank 1," LASL memo MP-3-99, Sept. 23, 1969 (unpublished).
- ³ P. W. Allison, C. R. Emigh, E. A. Meyer, D. W. Mueller and R. R. Stevens, Jr., "Operation of LAMPF 750 keV Injector," Proc. this conf.
- ⁴ P. W. Allison, C. R. Emigh and R. R. Stevens, Jr., "Initial Operation of the Beam Transport System in the LAMPF Injector Complex," Proc. 1970 Linac Conf., NAL, Sept. 1970.
- ⁵ D. A. Swenson, "Operation of the First Tank of LAMPF," Proc. 1970 Linac Conf., NAL, Sept. 1970.
- ⁶ M. A. Trump, D. R. Machen, M. A. Paciotti, E. J. Schneider and D. A. Swenson, "Beam Perturbation Measurements," Proc. 1970 Linac Conf., NAL, Sept. 1970.
- ⁷ D. A. Swenson, "Double Cavity Buncher Systems," LASL memo MP-3-86, May 16, 1968 (unpublished).
- ⁸ D. R. Machen, "A Computer Based, Data Acquisition and Control System for LAMPF Beam Diagnostics," Proc. 1970 Linac Conf., NAL, Sept. 1970.